# Accepted Manuscript

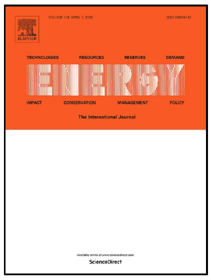


Integration of Distributed Energy Storage into Net-Zero Energy District Systems: Optimum Design and Operation

Mohammad Sameti, Fariborz Haghighat

PII: S0360-5442(18)30671-6

DOI: 10.1016/j.energy.2018.04.064

Reference: EGY 12703

To appear in: *Energy*

Received Date: 19 December 2017

Revised Date: 16 February 2018

Accepted Date: 11 April 2018

Please cite this article as: Mohammad Sameti, Fariborz Haghighat, Integration of Distributed Energy Storage into Net-Zero Energy District Systems: Optimum Design and Operation, *Energy* (2018), doi: 10.1016/j.energy.2018.04.064

# Integration of Distributed Energy Storage into Net-Zero Energy District Systems: Optimum Design and Operation

Mohammad Sameti*, Fariborz Haghighat*

Department of Building, Civil, and Environmental Engineering (BCEE),
Concordia University, Montreal, Quebec, Canada

## Abstract

A net-zero energy district is any neighborhood where the consumption of the buildings is offset by on-building generation on an annual basis. In this study, a net-zero energy district is identified among the set of optimal solutions and the effects of storage on its performance is investigated. It is assumed the model simultaneously optimizes the location of host buildings (energy generators), type of technologies and associated size, and the energy distribution network layout together with the optimal operating strategy. The optimization model addresses all technologies with a special focus on the effect of application of energy storage. Two types of energy storage are considered inside each building: thermal energy storage (hot water tank) and electrical energy storage (battery bank). The model is applied to the new part of a district energy system located in Switzerland. The best integrated district energy systems are presented as a set of Pareto optimal solutions by minimizing both the total annualized cost and equivalent $CO_2$ emission while ensuring the reliable system operation to cover the demand. The results indicated that selection of the proposed optimal district energy system along with the storage brings great economic and environmental benefits in comparison to all other scenarios (conventional energy system, stand-alone system, and net zero-energy without storage).

**Keywords:** $4^{th}$ generation; district; storage; distributed; optimal design; decentralized; MILP; net-zero energy

*Corresponding authors:
fariborz.haghighat@concordia.ca, mohammad.sameti@concordia.ca

## Nomenclature

**Latin symbols**

| | | | |
|---|---|---|---|
| $A$ | Surface area of PV ($m^2$) | $I$ | Carbon intensity (kg/kWh) |
| $E$ | Power flow (kW) | $X$ | Binary variable for CHP |
| $p$ | Price of energy carrier | $Y$ | Binary variable for pipeline connection |
| $C$ | Cost per unit production (€/kWh for all technologies except PV and (€/kWh.m² for PV) | $Z$ | Binary variable for chiller |
| $G$ | Nominal capacity (kW) | $U$ | Binary variable for boiler |
| $d$ | Distance (m) | $V$ | Visiting order |
| $O$ | Binary variable for chiller | $W$ | Binary variable for selling/purchasing power |
| $Q$ | Heat flow (kW) | $T$ | Binary variable for wire connection |
| $CT$ | Carbon tax (€/kWh) | $S$ | Solar irradiation (kW/m²) |
| $B$ | Binary variable for thermal storage | $R$ | Binary variable for battery bank |
| $SOC$ | State of the charge (kWh) | $F$ | Objective function |
| $r$ | Interest rate | | |

**Greek symbols**

| | | | |
|---|---|---|---|
| $\sigma$ | Percentage of heat loss | $\theta$ | Inclination angle |
| $\eta$ | Efficiency | $\Delta$ | Duration (hour) |
| $\zeta$ | Heat to power ratio | $\alpha$ | Interest rate |

**Subscripts and superscripts**

| | | | |
|---|---|---|---|
| tot | Total | K | Type of CHP unit |
| Inv | Investment | Sol | Solar |
| op | Operation | chil | Chiller |
| car | Carbon emission | S | Season |
| elec | Electricity demand | T | Period |
| pur | Purchased | grid | Utility grid |
| sel | Soled | Gas | Fuel (natural gas) |
| $i,j$ | Building number | Lo | Lower bound |
| PV | Photovoltaic array | Up | Upper bound |
| B | Boiler | used | Self-used energy |
| CHP | Cogeneration unit | eat | Heating demand |
| max | Maximum capacity | M | Number of chillers |
| n | Number | HS | Heat storage |
| BB | Battery bank | cost | Total annualized cost |
| emi | Emission | | |

**Abbreviations**

| | | | |
|---|---|---|---|
| COP | Coefficient of performance | DHC | District heating and cooling |
| CHP | Combined heat and power | CRF | Capital recovery factor |

## 1. Introduction

Similar to the electricity production system situated inside or close to end-users, district energy system can simultaneously supply power, heating, and cooling in an efficient way to cover the demands of local consumers [1]. Significant benefits are provided by such systems, namely saving primary energy by heat recovery, low heat and power transmission loss, and improved energy and exergy efficiencies [2, 3]. The rational design and operation strategy of district energy systems play a key role to achieve maximum economic benefits and provide best energy saving strategy. The design of a district energy system calls for the rational creation of its structure through choosing the suitable technologies from numerous alternatives together with the appropriate number and size of each equipment to reliably cover the energy demands of the end-users [4, 5]. Meanwhile, the best management strategy and load allocation for the selected technologies have great importance, which depends heavily on temporal variation of buildings energy requirements [6]. Energy simulation tools typically fail to take into consideration all the parameters simultaneously. For example, HOMER, a well-known tool has storage technologies including batteries, flywheels and hydrogen without any thermal energy storage. The tool has a limited number of thermal units that are typically simplified: CHP, boiler, and biomass [7]. Therefore, to perform such a complicated task, mathematical programming approaches have been employed for a wide range of applications to make informed decisions about the optimal design and management of district energy systems [8].Linear programming (LP) and mixed-integer linear programming (MILP) are the two most common approaches employed by the designers and engineers because the problem usually incorporates thousands of variables [9]. Vesterlund and Dahl [10] focused on the loop in the distribution network of a district. They introduced a new methodology to simplify the analysis of the complex networks with several loops to find the bottlenecks. In a study done by Wang et al. [11], an improved optimization model was proposed to provide smoother operation of cogeneration units by imposing a new constraint for power ramping. Carpaneto et al. [12] investigated integration of solar energy into existing districts to minimize the management cost by considering collector heat loss and produced power. Wang et al. [13] employed a conventional simple optimization algorithm to reduce the operation cost of pumping and heat exchanger in a high-rise apartment building. An operational optimization is carried out by Wang et al. [14] focusing on characteristics of the district energy system considering pumps with variable speed. A study on low-temperature district heating system is performed by Tunzi et al. [15] in which the operating temperature of the plate radiators is reduced. It also concluded that overall heat distribution losses and fuel consumption is lowered by 10%. In a similar work, Park et al. [16] found the optimized supply temperature in a secondary distribution network of a low district heating system. Supply temperature affects the costs related to heat loss, pumping energy, and required area of the heat exchangers and therefore an optimum solution exists that minimizes the total cost. Schweiger et al. [17] introduced a two level optimization model, which split the control problem into discrete and continuous sub-problems. The model is applied to optimize the thermal and hydraulic behavior of a district heating and cooling system. In another study based on decomposition technique, Sameti and Haghighat [4] developed a methodology to simultaneously optimize the design and operation of a tri-generation district. The authors showed the effectiveness of their model on a virtual case study focusing on supply and return temperatures as well as selecting components. In a study on district cooling, Khir and Haouari [18] developed a computational non-linear optimization model to achieve the optimum size of the chillers, cold thermal storage, and structure of the primary distribution pipeline. Temperature and pressure drops were also considered in their hydraulic model. Zhou et al. [19] carried out a comparative analysis of constant-efficiency and off-design characteristics for a tri-generation district to achieve lowest overall cost of the system. Powell et al. [20] introduced a dynamic optimization model to obtain the appropriate time of charging/discharging for a thermal energy storage and manage cooling and power load shifting. Jie et al. [21] investigated the variability of flow rates in both primary and secondary energy distribution networks on the pumping cost and on the cost associated with heat losses in an existing district. Jiang et al. [22] optimized the fuel consumption of an integrated system comprising of a wind turbine as one of the suppliers for an electric water heater together with a solar water heater and a gas-fired boiler. Ren et al. [23] put forward an optimization model to find the best operational management of a district power system composed of PV arrays, fuel cell, battery bank, and utility grid to achieve the most beneficial economic and environmental level. In a similar study done by Sameti and Haghighat [24], the capital cost of designing a new system is also taken into account where the interaction of heating and power is also analyzed. Fang et al. [25] developed a static model using genetic algorithm (GA) to optimize the district supply temperatures and load allocation among the plants based on the real-time end-user measurements. MILP could not tackle the problem due to non-convexity therefore the authors employed GA. Kim et al. [26] studied the connection of eleven district heating systems to minimize the total cost and maximize profits. However, their model should have included pumping cost because the pipelines connecting the districts are long and the pressure drop is a major issue. Zhen et al. analyzed the economic and environmental impact of a district integrated with a heat pump driven by seawater as the heat source for both heating and cooling [27].

It is however, important to mention that most of the aforementioned studies concentrate on matching supply and demands without considering any storage medium in their design or model. Moreover, energy storage in decentralized district energy systems has not been thoroughly studied especially when the design and operation of the storage system are accompanied by sizing, energy sources location, and load allocation of technologies implemented on the building. This paper addresses the aforementioned issues by presenting a comprehensive economic and environmental multi-objective optimization model for the investment planning of heat and power district energy systems emphasizing on the thermal and electrical storage. The set of optimal solutions opens up an opportunity to analyze the optimal design of a net-zero energy district and a stand-alone district, and investigate the effects of storage and energy exchange on cost and $CO_2$ emissions. Definition and analysis of net-zero energy district are totally new fields in the area of future sustainable districts where its simulation and optimization is carried out for the first time in this study.

## 2. Methodology

In this paper, the optimal design of the district energy system has been established based on a trade-off among two objective functions: total annualized cost and annual $CO_2$ emission. The total annualized cost, $F_{cost}$, is the sum of annual investment cost and the annual operating cost minus the income made by selling excess electricity to the grid. The optimization process tries to minimize the level of both functions as:

$$F_{pareto} = \min\,(F_{emi}, F_{cost}) \tag{1}$$

Hence, Bounded Objective Function (BOF) approach is employed to obtain the Pareto optimal solution. In this method, the lowest and the highest acceptable achievement levels for annual $CO_2$ emission is specified as $F_{emi}^{min}$ and $F_{emi}^{max}$ and the minimum of the cost function is obtained subject to previous constraints together with a new constraint as:

$$F_{emi}^{min} \leq F_{emi} \leq F_{emi}^{max} \quad (2)$$

which indicates only one point on the Pareto optimal frontier for a specific given reasonable interval. For a specific solution, a decision maker or governmental incentives may prefer one objective function to other one. In Eq. (1), sometimes absolute values of both objective functions are normalized by reference cases to keep their order of magnitudes the same. The reference case is considered as the optimal total annualized cost of a conventional district in which the boilers inside every building cover the heat demand and the electricity load is satisfied by the utility grid. However, in this study both environmental and economic objective functions are employed.

The optimization process is divided into four steps shown in Figure 1, which are solved iteratively within two different loops to constitute the Pareto optimal front. As illustrated in Figure 1, in the first step a value is assigned for the upper and lower bounds to form the single objective function optimization. In the second step, the design of the district technologies and/or their rated capacities is determined. In the third step, the pattern of the distribution heating and power network is established. The design of the heating and power networks covers a wide range of connections among the buildings. It can consist of several smaller sub-networks as well as no distribution network at all. Moreover, selection of equipment is widely varied while each building has the potential of accepting any type of generation or storage unit. The fourth step takes care of the optimal operation and load allocation of all technologies and storage systems. Information regarding updated variables for selection of equipment are passed back to the second step to get values that are closer to the optimal solution.

In this paper, the energy performance of a neighborhood is examined in which several options are available to cover its power and thermal demands. The implementation of on-building equipment combined with heating and power distribution networks and storage systems are considered. The district is composed of a number of buildings with given power and thermal demand profiles as well as the distances among the buildings. Figure 2a shows that each building can meet its heat requirements by a CHP unit, an individual supplementary boiler, and a thermal storage tank. A thermal storage tank is used in the case of showing heat surplus, which is consumed in subsequent periods. Both back-up boiler and CHP unit are driven by natural gas. A PV array, a CHP unit, and a battery bank can satisfy the electricity load. The excess electricity may be delivered back to the utility grid to generate profits or can be stored in the battery bank for succeeding utilizations. The utility grid also plays a role in providing electricity to the district to eliminate deficit electricity when there is not enough generation or the generation is not beneficial in some periods. Heat and electricity exchanges are possible among the buildings in the neighborhood through thermal and power transmission networks. As Figure 2b illustrates, the utilization of a central controller provides the entire buildings with management of the balance on the energy supply and demand. In other words, the district electricity requirements are not billed up to a point where it is covered by local power generation inside the neighborhood otherwise the electricity consumption is billed. Local controllers take care of the energy management inside each building as well as how much energy should be stored at any instant of the time. The input data to the optimization model and the outputs are given in **Figure 3**. All the decision variables listed in **Figure 3** are optimized based on the objective function given in Eq. (1).

### 2.1 Optimization model

Annual operation of the installed equipment is divided into three seasons and each day is partitioned into six periods as illustrated in **Table 1**. This division is done based on how close the demands are during successive hours. For example period III includes only one hour since the demand for this hour cannot be combined with other periods earlier or ahead of it. The hourly load is assumed to be constant for each period, however, other parameters such as solar irradiation is deemed as hourly basis. The revenue is defined as the income by selling electricity to the utility grid. The overall annualized cost is composed of the capital cost of technologies (CHP units, back-up boilers, thermal storage, battery bank, and PV array), cost of purchased electricity from the utility grid, cost of establishing the distribution network, cost for operation and maintenance of the district energy system. The environmental function considers $CO_2$ equivalent emission caused by the operation of back-up boilers and CHP units as well as the electricity purchased from the grid. Assuming short distances among the buildings, required power for pumping and therefore associated cost are negligible. The optimal solution of the distributed energy system described above insures that all constraints are satisfied i.e. all the installed technologies operate reliably and no reliability term is included in the objective functions.

The total cost, $F_{cost}$, is the sum of annual investment cost, $F_{cost}^{inv}$, and the annual operating cost, $F_{cost}^{op}$, minus the income made by selling excess electricity to the grid, $F_{cost}^{grid,s}$, (purchase of electricity, $F_{cost}^{grid,p}$, is already included in annual operating cost). The total annual cost for purchasing electricity, $F_{cost}^{grid,p}$, from the grid is calculated by multiplying the accumulated amount of the electricity in each period by the electricity tariff in that period.

$$F_{cost} = F_{cost}^{inv} + F_{cost}^{op} - F_{cost}^{grid,s} + F_{cost}^{grid,p} \tag{3}$$

The total investment cost, $F_{cost}^{inv}$, is composed of the capital costs for the PV arrays, the supplementary boilers, the CHP plants, together with the cost of pipeline network among the buildings and storage systems, which are amortized by multiplying the cost of each component as:

$$F_{cost}^{inv} = CRF^{PV}C^{PV}G^{PV}\sum_i A_i^{PV} + CRF^{B}C^{B}\sum_i G_i^{B} + \sum_k\sum_i CRF_k^{CHP}C_k^{CHP}G_k^{CHP}X_{i,k} + \sum_i\sum_j C^{pipe}d_{i,j}Y_{i,j} + CRF^{HS}C^{HS}\sum_i G_i^{HS} + CRF^{BB}C^{BB}\sum_i G_i^{BB} \tag{4}$$

In Eq. (4), the associated capital recovery factor (CRF) for each component is defined as:

$$CRF = r(1+r)^n((1+r)^n - 1)^{-1} \tag{5}$$

The annual operating costs consider the cost of fuel purchased to run back-up boilers and the CHP plants as well as the electricity purchased from the grid:

$$F_{cost}^{op} = \sum_t \sum_s \sum_i n_{s,t} \frac{Q_{i,s,t}^{B} p_{s,t}^{gas}}{\eta^{B}} + \sum_k \sum_t \sum_s \sum_i n_{s,t} \frac{p_{s,t}^{gas} E_{i,s,t,k}^{CHP}}{\eta_{k}^{CHP}} + F_{cost}^{grid,p} \quad (6)$$

The total electricity produced by the CHP technology is the sum of electricity used by the buildings and the electricity sold back to the grid to generate revenue.

Auxiliary boilers and CHP plants consume fuel to generate heat and power and therefore cause carbon emission. Moreover, the electricity purchased from the grid should be considered in the environmental objective function because thermal power plants emit carbon dioxide. The total $CO_2$ emission, $F_{emi}$, can be obtained by adding them:

$$F_{emi} = \sum_t \sum_s \sum_i n_{s,t} E_{i,s,t}^{grid} I^{grid} + \sum_t \sum_s \sum_i n_{s,t} \frac{Q_{i,s,p}^{B}}{\eta^{B}} I^{gas} + \sum_k \sum_t \sum_s \sum_i n_{s,t} \frac{E_{i,s,t,k}^{CHP}}{\eta_{k}^{CHP}} I^{gas} \quad (7)$$

**Table 2** lists all the design constraints considered in the optimization model for all candidate technologies.

Electricity demand for each building is the sum of the electricity purchased from the utility grid, the electricity generated by the PV arrays and the cogeneration, electricity transfer among the buildings, and the battery bank:

$$E_{i,s,t}^{elec,tot} = E_{i,s,t}^{grid} + E_{i,s,t}^{PV,used} + \sum_k E_{i,s,t,k}^{CHP,used} + E_{i,j,s,t}^{EX} + E_{i,s,t}^{BB} \quad (8)$$

$$E_{i,j,s,t}^{EX} = E_{j \rightarrow i,s,t} - E_{i \rightarrow j,s,t} \quad (9)$$

Heat requirements can be supplied through the heat generated by back-up boilers and/or the CHP units, heat exchange among the buildings in the district, and the thermal energy storage as:

$$Q_{i,s,t}^{heat} = Q_{i,s,t}^{B} + \sum_k Q_{i,s,t,k}^{CHP} + Q_{i,j,s,t}^{EX} + Q_{i,s,t}^{HS} \quad (10)$$

$$Q^{EX}_{i,s,t} = (1 - \sigma)Q_{j \to i,s,t} - Q_{i \to j,s,t} \tag{11}$$

In the both previously mentioned heat and electricity balance equations, the power and heat flow for storage systems can be positive or negative, following the convention that negative flow implies charging and positive one means discharging, one can write:

$$Q^{HS}_{i,s,t} = Q^{HS,dis}_{i,s,t} / \eta^{HS}_{dis} - \eta^{HS}_{ch} Q^{HS,ch}_{i,s,t} \tag{12}$$

$$E^{BB}_{i,s,t} = E^{BB,dis}_{i,s,t} / \eta^{BB}_{dis} - \eta^{BB}_{CH} E^{BB,ch}_{i,s,t} \tag{13}$$

The energy balance equation for the thermal storage system states that the total amount of available heat in the tank is equal to the amount of heat stored in the previous period plus the heat flow directed towards the tank in the current period minus the heat flow that is released to cover the heat load:

$$SOC^{HS}_{i,s,t} = \eta^{HS} SOC^{HS}_{i,s,t-1} - Q^{HS}_{i,s,t} \tag{14}$$

The same description can be applied to the battery bank:

$$SOC^{BB}_{i,s,t} = \eta^{BB} SOC^{BB}_{i,s,t-1} - E^{BB}_{i,s,t} \tag{15}$$

The optimization model developed above is general, flexible, and applicable to any district with any size. In fact, for large districts and/or hourly input data the model can efficiently be solved by taking advantage of the decomposition technique (see Figure 3). Because both economic and environmental objective functions in Eq. (1) are convex and the linear combination is also convex, the weighting function approach can explore the whole Pareto front [28].

## 3 Illustrative example

A numerical study is illustrated in this section with seven residential and office buildings situated in Risch Rotkreuz, Switzerland. Schematics of the district energy system is illustrated in Figure 4. The area is under construction and is going to be completed by the year 2020. Therefore, the new district opens up an opportunity to investigate and evaluate various sustainable and beneficial designs and scenarios. Besides the topology of the district, other necessary input data for the optimization model is explained in the following sections:

### 3.1 Energy demand

Detailed information about energy requirements, for at least one year, is essential for an accurate optimal design and planning of a district energy system. Table 3 and Table 4 list the representative electricity and heating consumption profiles for the periods defined earlier in Table 1 for each of the seven buildings used in the case study. It is important to mention that the electricity consumption profiles does not include the electricity required by the compression chillers for cooling. However the purpose of the current study is to develop an optimized design for heating and power of the district (cooling equipment are not included), the power required for the compression chillers can be easily taken into account as part of the required electricity (power) of the district energy system or part of the excess electricity.

### 3.2 Electricity and fuel tariffs

Another essential input to the model is the market data for electricity buy-back price by CHP plants and PV units together with the purchase price of electricity from the utility grid which are all listed in Table 5 for each period. It is also assumed that natural gas is consumed both by the boiler and the CHP plants where based on 1 kWh produced heat, the fuel tariff is 0.054 €/kWh [29] and the equivalent $CO_2$ emission is 0.184 kg considering the lower heating value of the fuel. Associated $CO_2$ emission for every 1 kWh of generated electricity in the conventional power plant which is purchased from the grid is 0.781 kg [8, 4]. It is assumed that the electricity network can at any given instant absorb the excess power provided by the district system.

### 3.3 Available technologies

Various options for technologies and network design along with their technical characteristics and prices are listed in Table 6. There are six options for CHP in Figure 6 however all of them have the same electrical efficiency and heat-to-electricity ratio (HER). It should be mentioned that the size of the back-up boiler is a continuous decision variable and can get any value between 0 kWh and 30 kWh. The optimization model also assumes that all the conversion efficiencies for CHP plants, boiler, PV array, and storage systems are fixed, however, application of CHP technologies in time-varying demand environments along with their partial load efficiency variations signifies the importance of modeling these technologies with load dependent efficiencies. An examples of the models using constant efficiencies for CHP technologies is given by Milan et al [31]. Moreover, PV module temperature is a parameter that has great influence in the behavior of a PV system, as it modifies system efficiency and output energy. In addition to this, the atmospheric parameters such as irradiance level, ambient temperature, wind speed, dirt/dust and the particular installing conditions have influence, too. The error introduced by considering constant efficiencies is negligible for model with high-level design [19]. Lifetime of all equipment is considered to be 20 years with the annual interest rate of 7.5% for capital costs.

### 3.4 Available PV area and solar irradiation

Table 7 gives the available space to install the PV units on top of each building, while Figure 7 provides the hourly solar irradiation for three typical days in the periods defined earlier. It should also be mentioned that the solar radiation input to for the PV units is based on an hourly basis. All the roof surfaces are horizontal and flat and the areas given in Table 7 are virtually 20% less than the total available area on the top of each building.

### 3.5 Setting of scenarios

Four different scenarios are envisaged and optimized to find a set of optimal solutions in which a net-zero energy district is recognized and the effects of storage is analyzed. A comparison is also made with a stand-alone district energy system. The first scenario is defined as a reference scenario where no poly-generation system and no energy network are employed. This scenario is then compared to the modern district energy systems with poly-generation and heat/power exchange. Since the evaluation of the impact of energy storage is one of the purpose of the current study, scenarios 2 and 3 describe two modern district energy systems in the presence/absence of thermal energy storage and battery bank.

**Scenario 1 (*conventional district*):** A conventional system is simulated where the utility grid meets the electrical demand and gas-fired boilers provide the heating demand. No other technologies including thermal storage systems and distribution network is considered in this scenario.

**Scenario 2 (*district energy system without storage*):** All technologies (PV and CHPs) together with the back-up boilers but not storage systems can be installed in the district, and the buildings can interact with each other by electrical connections and pipelines to exchange energy and cover their loads when applicable. District is also connected to the utility grid to buy and sell electricity. A net zero-energy district can be recognized among the solutions.

**Scenario 3 (*district energy system with storage*):** All technologies (PV, CHPs, boilers) including electrical and thermal energy storage can be installed in the district, and the buildings can exchange heat and electricity. Buildings may provide and get electricity to/from the utility grid. A net zero-energy district can be recognized among the solutions.

**Scenario 4 (*stand-alone district*):** The district works as a stand-alone system and is not connected to the utility grid. PV units, CHP plants, supplementary boilers, thermal energy storage tank, and battery bank can be installed in the district, and the buildings may exchange heat and electricity.

The proposed MILP optimization model is coded in General Algebraic Modeling System (GAMS) CPLEX [5] and has been solved for the aforementioned scenarios to get optimal set of solutions. The GAMS is a modeling tool for mathematical programming and optimization purposes. The tool is used to model and solve linear, nonlinear, and mixed-integer linear and nonlinear optimization problems. The tool is very well-known in the area of energy optimization since it allows changes to be made in model specifications simply and safely while allowing unambiguous statements of algebraic relationships.

## 4 Results and discussions

The simulation results showed that for a conventional district (scenario 1) an optimized solution costs 12 000 € per year where significant portion of that is the operational cost (almost 70%). Such a system emits more than 52 300 kg $CO_2$ per year where 28 000 kg $CO_2$ is associated with the gas boiler and 24 300 kg $CO_2$ is from purchasing electricity from the utility grid and associated with the fuel burns in the large power plants. All the decision variables remain the same in all scenarios but the *optimal* solution to the optimization problem contains only *one* point. It means that no other solution exist with lower cost/emission than that point. In other words, increasing the cost (by implementation of other technologies) results in higher emission. This point is not illustrated in the graphs in this section because it exceeds the limit of the axes. The result of optimization model for other scenarios is expressed as a number of feasible solutions which reflects the different capacities of the CHP, boiler, thermal storage, battery bank, and PV as well as the optimal network structure and operation of the generation units. For most of the solutions, the $CO_2$ emission interval is set to 1000 kg or 500 kg as it can be seen from the results in Figures 8 to 10.

For the grid connected district without any storage system installed (scenario 2), the best solution with respect to the total annual cost needs -1 830 € for designing of the system which emits 31 730 kg $CO_2$ per year. This point on the Pareto front shows 40% improvement in the emission rate while 150% improvement is achieved in the total annual cost compared to conventional district. The negative sign implies that operation of equipment in the district generates high income i.e. the designed district is an "energy-plus" district energy system. The design is capable of compensating all its annual investment and operational costs by selling electricity to the utility grid to provide income for the buildings. The best solution associated with the emission requires 1 325 € per year and emits 20 700 kg $CO_2$. This solution leads to 89% saving in the cost together with 61% reduction in the $CO_2$ release. Both best solutions with regard to each objective functions are located at the ends of the

Pareto front and marked with red color. The dashed line in Figure 8 forms a border between the districts receiving an income and the required budget for the design and operation. This threshold defines the “net-zero energy” district energy system which produces 22 500 kg $CO_2$ per year. The solutions on the left-hand side of the Pareto front are compact and close to each other. For instance, by earning less than only 20 € per year, the $CO_2$ emission increases rapidly by 1000 kg (from 31 000 kg to 32 000 kg). However, the situation is completely different on the right-hand side of the dashed line where the solutions are more distant and there is a gap among them.

Table 8 shows that only one big CHP unit (10 kW) is implemented in the district and located in building B1 and its capacity is not enough to electrify all the buildings therefore PV units serve as a secondary power generator. Further analysis of the optimal lay-out in Figure 11, illuminates how the energy produced by the sole generator is distributed among the buildings through the network. In this scenario, all the buildings are connected to one united pipeline system. The direction of the flow in Figure 11 is counterclockwise because the distance between buildings B1 and B2 are less than that between buildings B1 and B7. In other words, the shorter path is followed by the optimization procedure to lower the pipeline costs associated with building a new distribution network.

For the grid connected district with storage systems installed (scenario 3), the best solution with respect to total annual cost generates -1 920 € income and emits 29 000 kg $CO_2$ per year. It shows an improvement of 5% in cost and 9% in emission in comparison with the district without any thermal storage. The best solution associated with the emission requires 1 418 € per year and emits 18 500 kg $CO_2$. In this case, the cost of the system is a little higher but there is 18% less annual emission compared to the case without storage systems. The net-zero energy district in scenario 3, produces 20 800 kg $CO_2$ per year which is 15% lower than that of scenario 2.

For a net-zero energy district with storage systems (scenario 3), Table 9 lists all the technologies implemented in each building as well as their capacities. Electrical energy storage (battery bank) is selected by the optimization procedure in all buildings with the same size. Moreover, all the buildings are equipped with PV units to their maximum available space. The results show that implementation of more low-capacity heat generation units (5 units) is more profitable than installation of less number of larger units (especially CHP plants) with higher capacity. Analysis of the optimal structure of pipelines in Figure 12 shows that the district consists of 4 subnetworks: (i) Buildings B2, B3, and B4 which are connected to each other, (ii) building B6 and B7 are linked together, (iii) Building B1 alone, (iv) Building B5 alone. The results show that other buildings are isolated from the distribution network and have their own individual technologies. For the buildings which receive thermal energy through the distribution network (i.e. buildings B3, B4, and B6), no heat generation unit is implemented inside them which shows the effectiveness of heat exchange among the consumers. For the isolated buildings, thermal energy storage with higher capacity is installed to store excess heat in a case that CHP units is generating and selling electricity to the utility grid. Three thermal storage tanks inside three buildings with 1.77 kWh capacity balance the mismatch between demand and received energy in the isolated buildings at some periods of time. On the other hand, isolated buildings have the same capacity for battery as other buildings because they are connected through wires to other producers and can receive extra energy to store. Considering any two points with the same emission on Figure 8 and Figure 9, this conclusion is drawn that implementation of energy storage lessens the cost by almost 1 000 € per year. For example, for the annual $CO_2$ emission equal to 22 000 kg, storage system is able to decrease the annual cost from 320 € to -700 € implying 318% saving. The same conclusion can be drawn by comparison between the points with same total annual cost. For instance, for 1 000 € income per year, adding storage causes more than 1 500 kg reduction in $CO_2$ emission. Therefore, utilization of energy storage is profitable in both economic and environmental aspects.

For a stand-alone district (scenario 4), no utility grid exists and all the electricity is consumed internally. Since there is no opportunity to sell electricity, no income is provided and energy storage can play a significant role in smoothing the load. As Figure 10 depicts, the lowest cost to design such a district is 8 600 € per year where the $CO_2$ emission is around 24 500 kg. The highest cost corresponds to a point with more than 19 000 kg annual $CO_2$ emission and 10500 € for overall design and operation costs. By selecting two points with the same emissions as two net-zero energy systems discussed earlier i.e. 20 800 kg and 22 500 kg for systems with and without storage, respectively, a comparison can be made for the costs. To reach the same emission as the second scenario an extra 9 300 € should be payed per year while for the third scenario and annual payment of 10 000 € should be met. For the configuration with lower cost (9 300 €), the list of implemented technologies in the district are summarized in Table 10. It can be seen that no heat distribution network exists among the buildings because there is no revenue to cover the costs of pipelines. The same explanation can be given for the area of the PV units where none of the buildings are equipped with them. All the buildings are isolated and host both boiler and CHP plants together with thermal and electrical storage systems to balance the mismatch between supply and demand profiles. It is important to mention that electrical connections among the buildings (electrical distribution network) still remains because unlike the pipeline, no cost is incurred for building with such electrical network. In fact, none of the optimal solutions for a stand-alone system requires heating connections among the buildings.

A comparison for purchased and sold electricity are given in Figures 13 and 14 for two net-zero energy districts. For the system without storage, PV units take the role of supplying the major part of the electricity demand as well as providing income. However, when the storage system is implemented, the share of electricity produced by CHP plants is raised considerably because the excess energy can be stored in the battery bank inside each building or exported to other buildings to be used or to improve the charge status of batteries implemented in those buildings. This share includes both the energy injected to the grid and the energy used internally in each buildings.

The state of the charge for thermal storage for all the buildings in the district with thermal storage is illustrated in Figure 15. Building B1 has the higher level of charge because it is supplied by both boiler and CHP unit and it is not connected to the thermal distribution network. Therefore, the excess energy cannot be exported to other buildings through the pipelines and should be stored. Unlike building B1, buildings B2, B3, and B4 creates a sub-network and provides the opportunity to export and receive heat. Hence, their state of the charge has the least levels among other storage systems.

Unlike the heat storage, the trend for battery bank storage level Figure 16 is virtually the same for all the buildings because there is an opportunity for the district to deliver the electricity back to the grid and generate income. Because a CHP unit with 5 kW capacity is installed in building B7, the excess electricity is exported to other consumers and therefore its level of charge is lowest in comparison with other battery banks implemented in the neighborhood.

In order to check the hourly energy balance, buildings B1 and B7 are selected and their hourly production and consumption are illustrated in Figures 17 and 18. The electricity demand curve sometimes drops below the CHP generation curve because some of the energy is transferred to other buildings and/or the battery bank is being charged.

Table 11 summarizes a comparison for the cost and $CO_2$ emission for some specific points characterizes each scenario. These points are basically the extreme points of the Pareto optimal frontier (lowest cost or emission) or the net-zero district for the two scenarios.

## 5 Conclusions

A comprehensive MILP optimization model is developed to optimize the design and operation of a new district, and implemented under four scenarios.

- A conventional grid-connected district with only boilers inside the buildings: This scenario has the highest cost and $CO_2$ emission which costs 12 000 € and emits 52 300 kg $CO_2$ per year.
- A grid-connected district with heat and electricity exchange and without any storage system: a net-zero energy district is recognized in the Pareto front which offers 56% decrease in emission compared to conventional district. The optimal topology of the case without storage has only one network where all the buildings are connected to each other through the shortest path.
- A grid-connected district with heat and electricity exchange and storage system: a net-zero energy district is recognized in the Pareto front which offers 60% decrease in $CO_2$ release. Structure of the system with storage has three sub-networks because releasing and storing of energy makes the buildings less independent of receiving and exporting to other buildings. With the same total annual emission, a district with storage provides more income (or costs less) compared to the district without

storage. Likewise, for the same total annual cost, a district with storage releases more $CO_2$ in comparison with the district without storage.

- For a stand-alone district, all the buildings are thermally isolated for all the optimal solutions in the Pareto front but there are still electrical connections among the buildings. The lowest cost of a stand-alone system costs 28% less per year compared to the conventional district where the $CO_2$ emission is reduced by 53%. The highest cost corresponds to a point with more than 63% decrease in annual $CO_2$ emission and 13% saving in overall design and operation costs.

Therefore, the district energy system with storage provides the best solution regarding both environmental and economic issues. Implementation of storage not only smooth the load allocation but also generates more income by selling electricity through suitable response to the heat and power demand. It is recommended for the future work to study the optimal location of power generation units in a centralized district and compare the results with a similar decentralized district. Also, it would be a good idea if a methodology is proposed to combine both prediction and optimization at the same time [35].

## Acknowledgement

Authors would like to express their gratitude to the Natural Sciences and Engineering Research Council of Canada and Concordia University for supporting this research and Miss. Farinaz Haghighat for her valuable comments and suggestions.

## References

[1] Y. Yang, S. Zhang and Y. Xiao, "An MILP (mixed integer linear programming) model for optimal design of district-scale distributed energy resource systems," *Energy,* vol. 90, pp. 1901-1915, 2015.

[2] M. Sameti and F. Haghighat, "Optimization approaches in district heating and cooling thermal network," *Energy and Buildings,* vol. 140, no. 1, pp. 121-130, 2017.

[3] S. S. Bahari, M. Sameti, M. H. Ahmadi and M. S. Haghgooyan, "Optimisation of a combined Stirling cycle–organic Rankine cycle using a genetic algorithm," *International Journal of Ambient Energy,* vol. 37, no. 4, pp. 398-402, 2016.

[4] M. Sameti and F. Haghighat, "A two-level multi-objective optimization for simultaneous design and scheduling of a district energy system," *Applied Energy,* p. Article in Press, 2017.

[5] M. Sameti, "Electrical Energy Efficient Building through Distributed Generation," *International Journal of Renewable Energy Research,* vol. 4, no. 3, pp. 777-783, 2014.

[6] B. Talebi, F. Haghighat, P. Tuohy and P. Mirzaie, "Validation of a community district energy system model using field measured data," *Energy ,* Article in Press.

[7] R. Sena and S. C. Bhattacharyya, "Off-grid electricity generation with renewable energy technologies in India: An application of HOMER," *Renewable Energy,* vol. 62, pp. 388-398, 2014.

[8] E. D. Mehleri, H. Sarimvais, N. C. Markatos and L. G. Papageorgiou, "A mathematical programming approach for optimal design of distributed energy systems at the neighbourhood level," *Energy,* vol. 44, pp. 96-104, 2012.

[9] W. Wang, X. Cheng and X. Liang, "Optimization modeling of district heating networks and calculation by the Newton method," *Applied Thermal Engineering,* vol. 61, pp. 163-170, 2013.

[10] M. Vesterlund and J. Dahl, "A method for the simulation and optimization of district heating systems with meshed networks," *Energy conversion and management,* vol. 89, pp. 555-567, 2015.

[11] H. Wang, E. Abdollahi, R. Lahdelma, W. Jiao and Z. Zhou, "Modelling and optimization of the smart hybrid renewable energy for communities (SHREC)," *Renewable Energy,* vol. 84, pp. 114-123, 2015.

[12] E. Carpaneto, P. Lazzeroni and M. Repetto, "Optimal integration of solar energy in a district heating network," *Renewable Energy,* vol. 75, pp. 714-721, 2015.

[13] W. Wang, X. Cheng and X. Liang, "Optimization modeling of district heating networks and calculation by the Newton method," *Applied Thermal Engineering,* vol. 61, pp. 163-170, 2013.

[14] H. Wang, H. Wang, Z. Haijian and T. Zhu, "Optimization modeling for smart operation of multi-source district heating with distributed variable-speed pumps," *Energy,* vol. 138, no. 1, pp. 1247-1262, 2017.

[15] M. Tunzi, R. Boukhanoul, H. Li, S. Svendsen and A. Ianakiev, "Improving thermal performance of an existing UK district heat netwrok: a case for temperature optimization," *Energy and Buildings,* p. Article in Press, 2017.

[16] B.-S. Park, M. Imran, I.-Y. Hoon and M. Usman, "Thermo-economic optimization of secondary distribution network of low temperature district heating network under local conditions of South Korea," *Applied Thermal Engineering,* vol. 165, pp. 117-133, 2017.

[17] G. Schweiger, P.-O. Larsson, F. Magnusson, P. Lauenburg and S. Velut, "District heating and cooling systems - Framework for Modelica-based simulation and dynamic optimization," *Energy,* vol. 137, pp. 566-578, 2017.

[18] R. Khir and M. Haouari, "Optimization models for a single-plant District Cooling System," *European Journal of Operational Research,* vol. 247, pp. 648-658, 2015.

[19] Z. Zhou, P. Liu, Z. Li, E. N. Pistikopoulos and M. C. Georgiadis, "Impacts of equipment off-design characteristics on the optimal design and operation of combined cooling, heating and power systems," *Computers and Chemical Engineering,* vol. 48, pp. 40-47, 2013.

[20] J. S. K. Kody M Powell and K. K. J. L. M. J. D. H. a. T. F. E. Wesley J. Cole, "Thermal energy storage to minimize cost and improve efficiency of a polygeneration district energy system in a real-time electricity market," *Energy,* vol. 113, pp. 52-63, 2016.

[21] P. Jie, N. Zhu and D. Li, "Operation optimization of existing district heating systems," *Applied themal engineering,* vol. 78, pp. 278-288, 2015.

[22] X. Jiang, Z. Jing, Y. Li, Q. Wu and W. Tang, "Modelling and operation optimization of an integrated energy based direct district water-heating system," *Energy,* vol. 64, pp. 375-388, 2014.

[23] H. Ren, Q. Wu, W. Gao and W. Zhou, "Optimal operation of a grid-connected hybrid PV/fuel cell/battery energy system for residential applications," *Energy,* vol. 113, pp. 702-712, 2016.

[24] M. Sameti and F. Haghighat, "4th generation decentralized district energy system: development of an optimization model for design and planning," *Renewable Energy,* p. Article in Press, 2018.

[25] T. Fang and R. Lahdelma, "Genetic optimization of multi-plant heat production in district heating networks," *Applied Energy,* vol. 159, pp. 610-619, 2015.

[26] U. S. Kim, T. C. Park, L.-H. Kim and Y. K. Yeo, "Optimal operation of the integrated district heating system with multiple regional branches," *Korean Journal Chemical Engineering,* vol. 27, no. 1, pp. 6-18, 2010.

[27] L. Zhen, D. M. Lin, H. W. Shu and S. Jian, "District cooling and heating with seawater as heat source and sink in Dalian," *Renewable energy,* vol. 32, no. 15, pp. 2603-2616, 2007.

[28] M. K.M., Nonlinear multiobjective optimization, Kluwer Academic, 1998.

[29] S. Obara, "Equipment arrangement planning of a fuel cell energy network optimised for cost minimisation," *Renewable Energy ,* vol. 32, pp. 382-406, 2007.

[30] T. Falke, S. Krengel, A.-K. Meinerzhagen and A. Schnettler, "Multi-objective optimization and simulation model for the design of distributed energy systems," *Applied Energy,* p. Article in Press, 2016.

[31] C. Milan, C. Bojesen and M. P. Nielsen, "A cost optimization model for 100% renewable residential energy supply systems," *Energy,* vol. 48, no. 1, pp. 118-127, 2012.

[32] H. Ren, W. Gao and Y. Ruan, "Economic optimisation and sensitivity analysis of photovoltaic system in residential buildings.," *Renewable Energy ,* vol. 34, pp. 883-889, 2009.

[33] I. Staffell, "Purchase cost of condensing boilers in the UK," 2008.

[34] M. De Paepe, P. D'Herdt and D. Mertens, "Micro-CHP systems for residential applications," *Energy Conversion and Management ,* vol. 47, pp. 3435-3446, 2006.

[35] M. Sameti, M. A. Jokar and F. R. Astaraei, "Prediction of solar Stirling power generation in smart grid by GA-ANN model," *Int. J. Computer Applications in Technology,* p. In Press, 2017.

## Figures

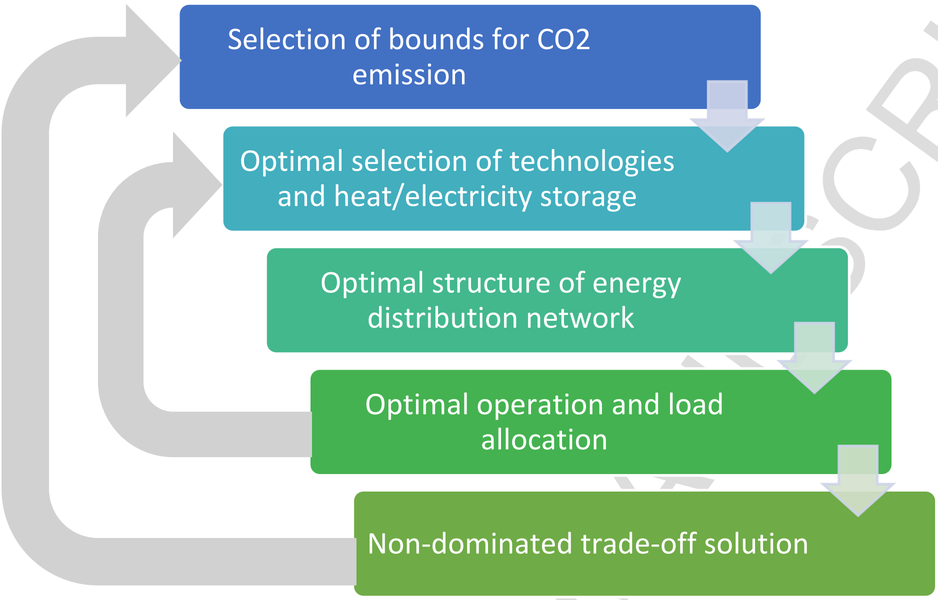


**Figure 1** Process of the proposed optimization model.

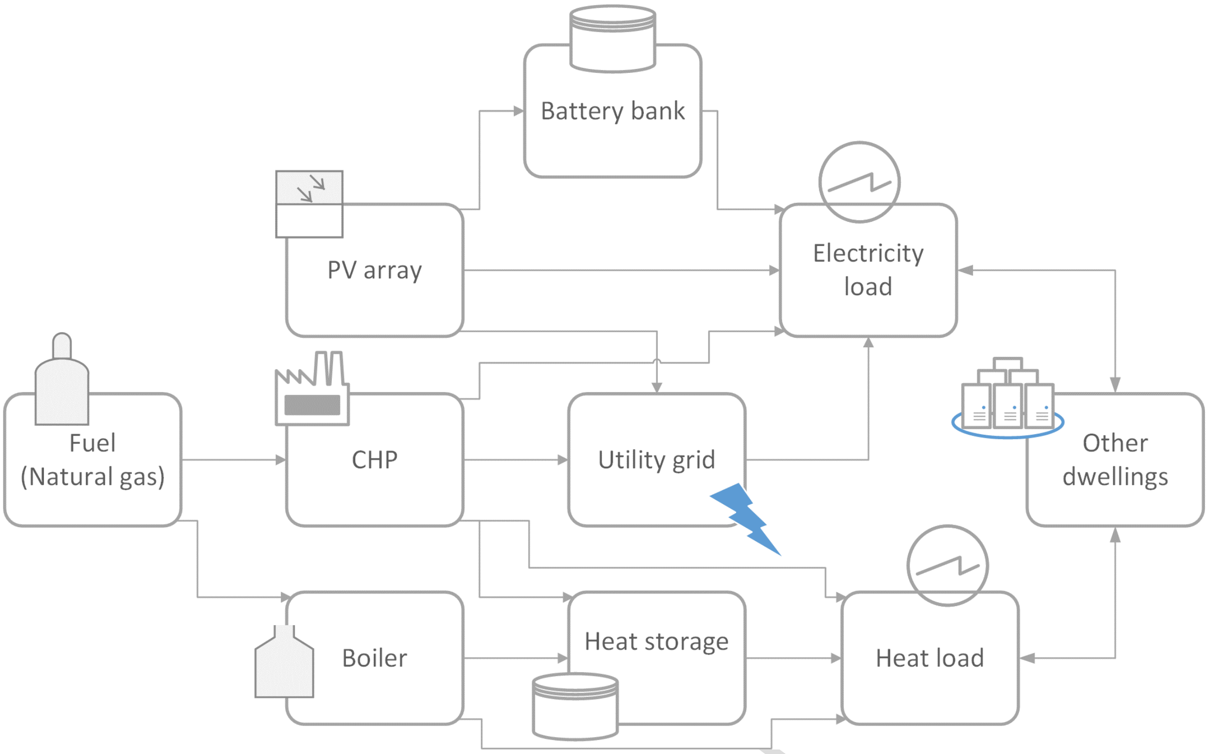


(a)

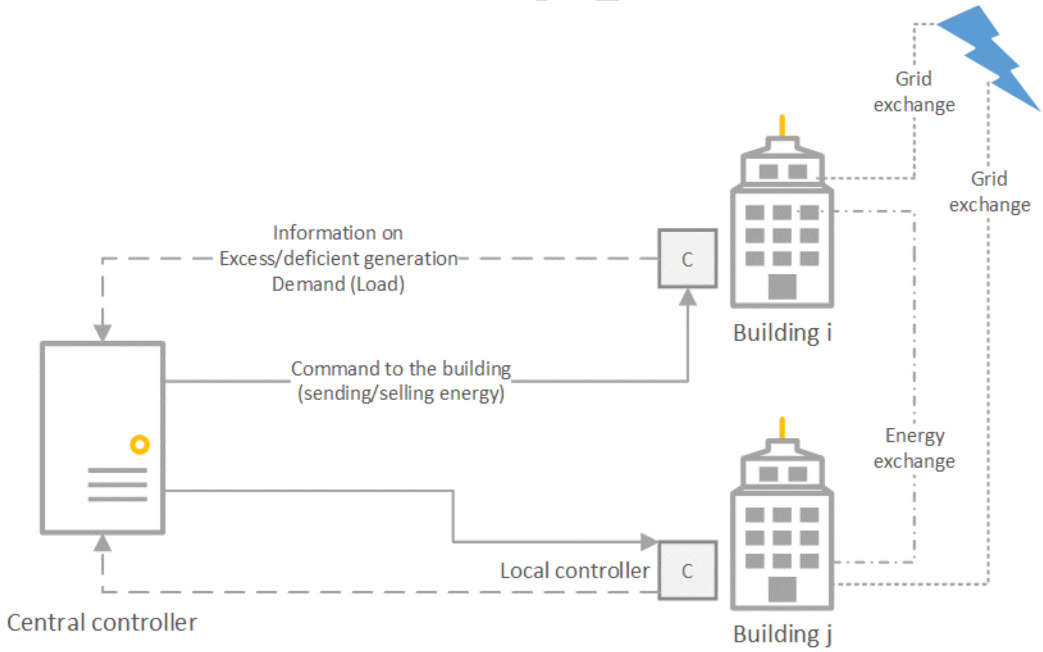


(b)

**Figure 2** Proposed (a) configuration and (b) management of the neighborhood

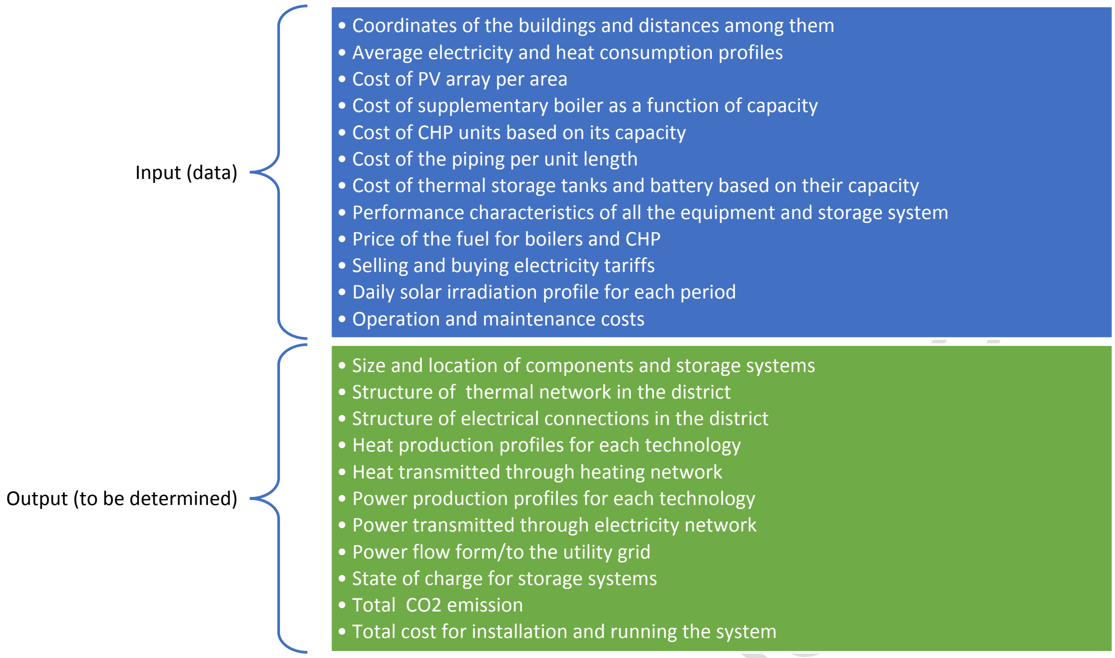


**Figure 3** Overview of the required data in the model and its output


**Figure 4** Geographic layout of the buildings in Suurstoffi district

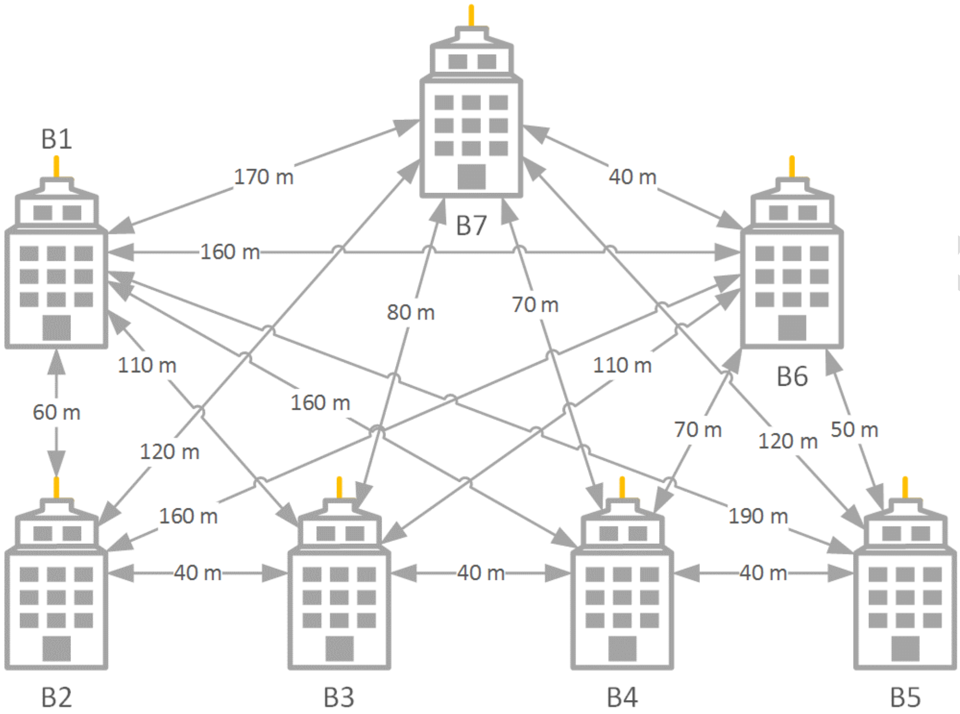


**Figure 5** Relative coordinates and distances among of the buildings in Suurstoffi district

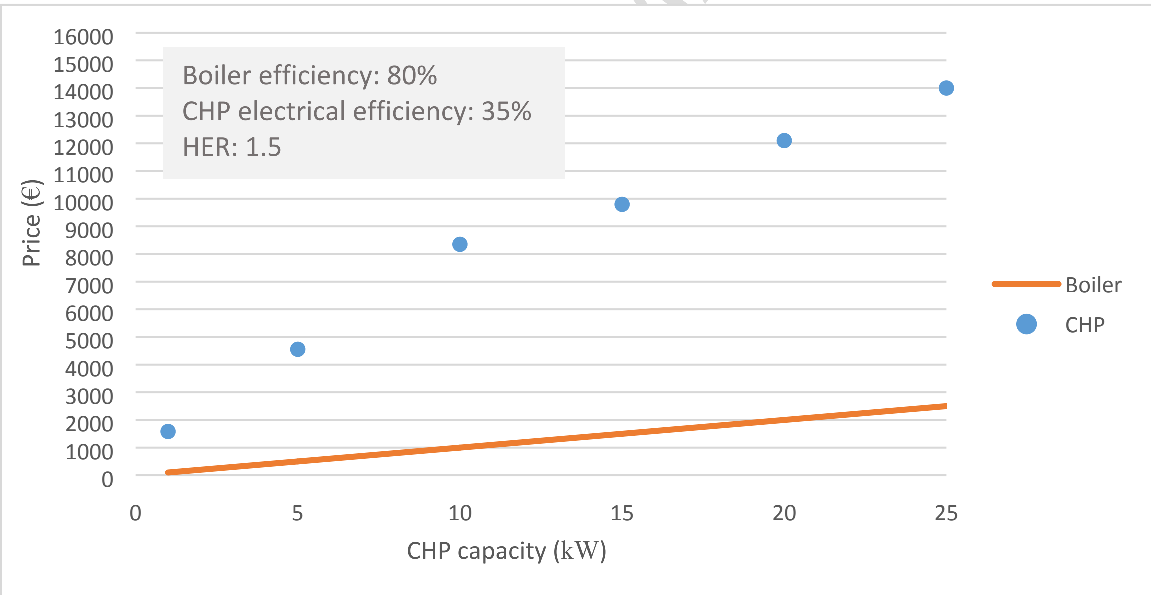


**Figure 6** Capital cost and technical characteristics of CHP and back-up boiler [32, 33, 34]

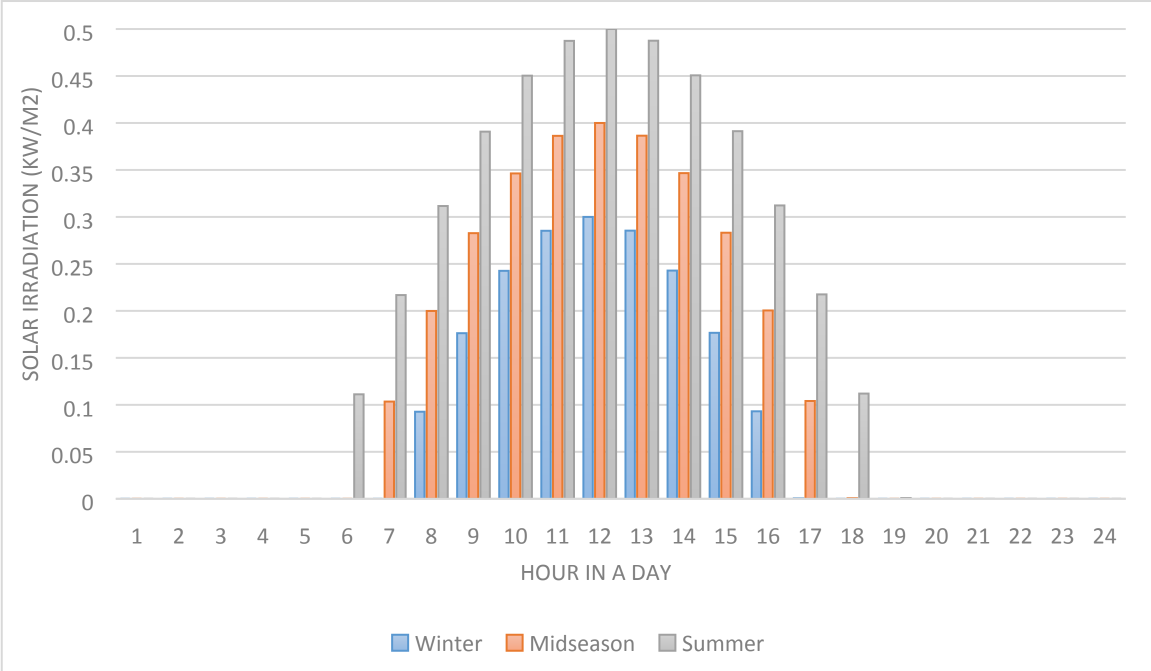


**Figure 7** Hourly irradiation for typical days for each season (January 1st for winter, April 1st for mid-season, and July 1st for summer all for horizontal surface or $\theta = 0°$)

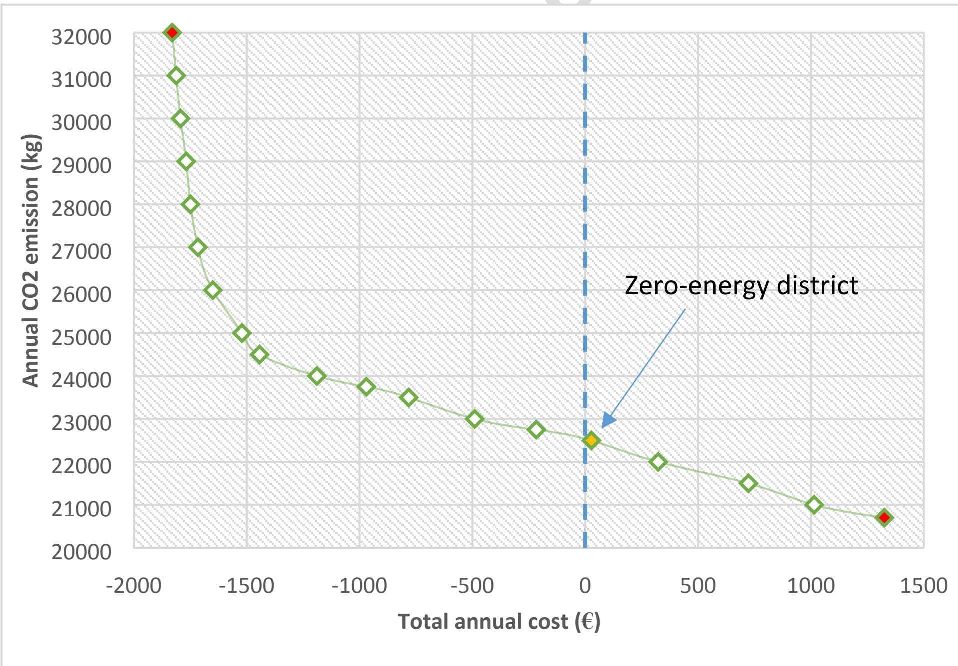


**Figure 8** Pareto efficient solutions for design of the district energy system (grid connected without storage)

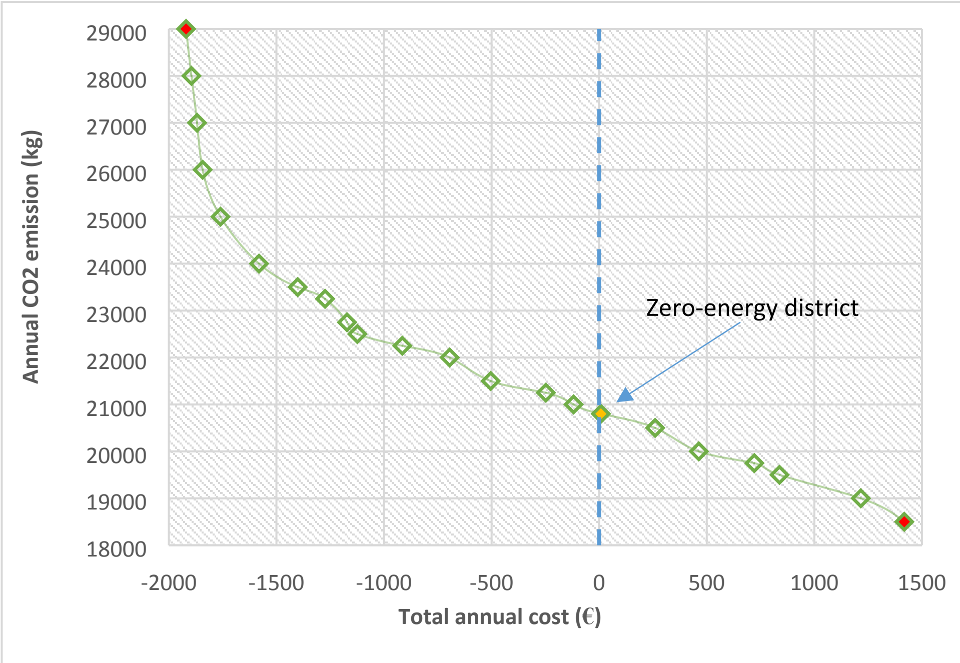


**Figure 9** Pareto efficient solutions for design of the district energy system (grid-connected with storage)

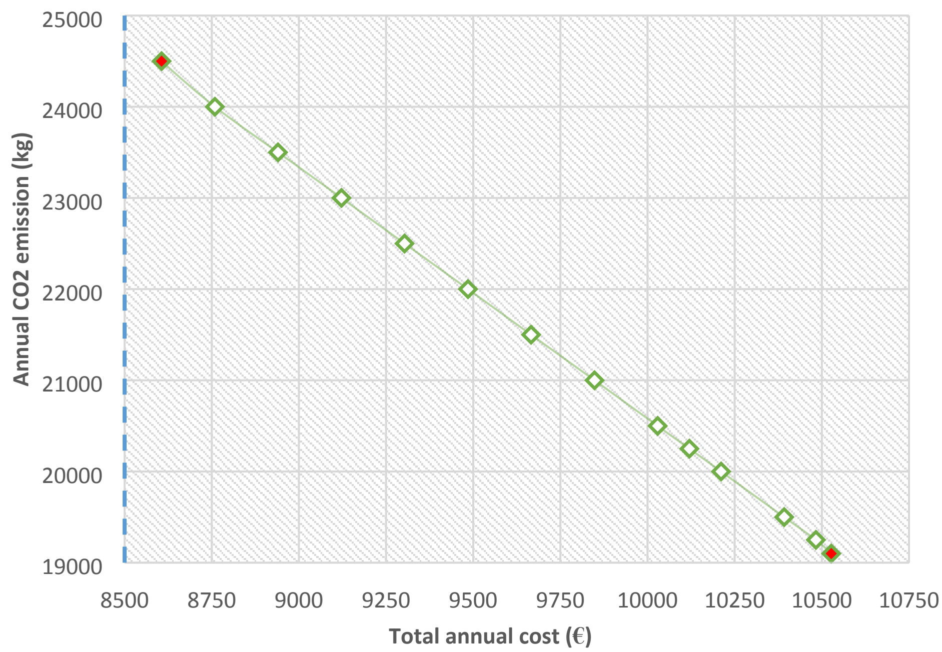


**Figure 10** Pareto efficient solutions for design of the district energy system (stand-alone)


**Figure 11** Optimal lay-out of the net-zero energy district without storage


**Figure 12** Optimal lay-out of the net-zero energy district with storage

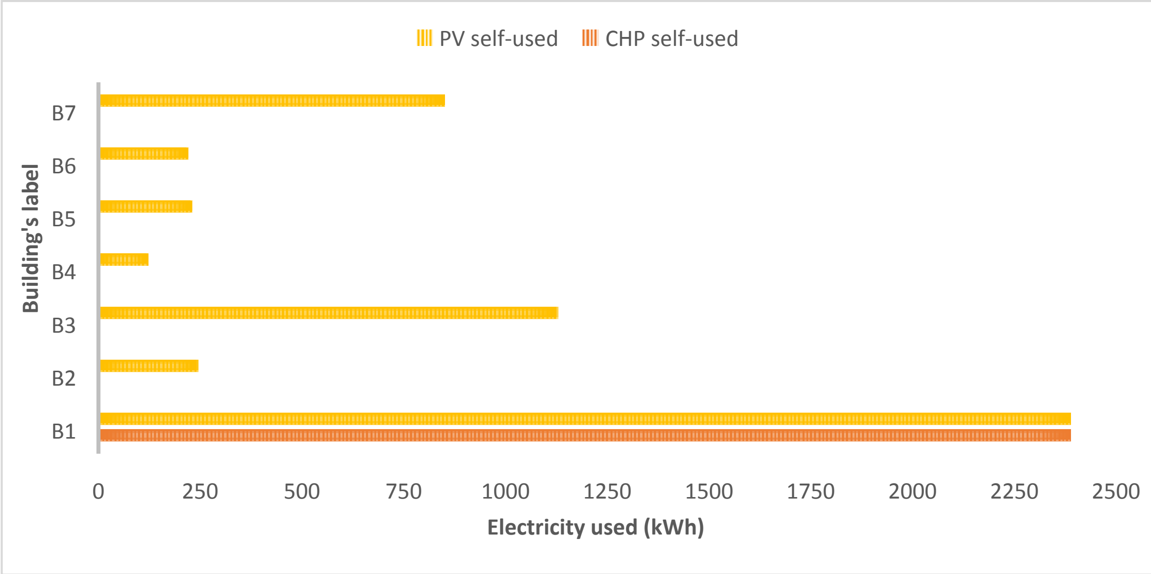


**(a)**

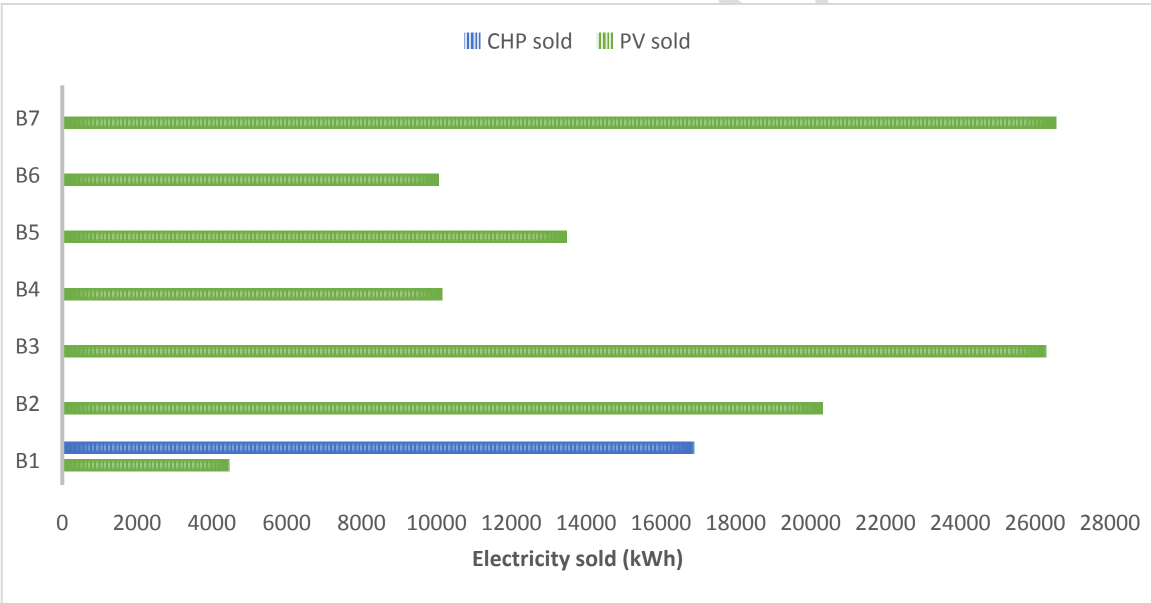


**(b)**

**Figure 13** Power energy balance throughout the year for net-zero energy district without storage based on (a) self-used and (b) sold energy

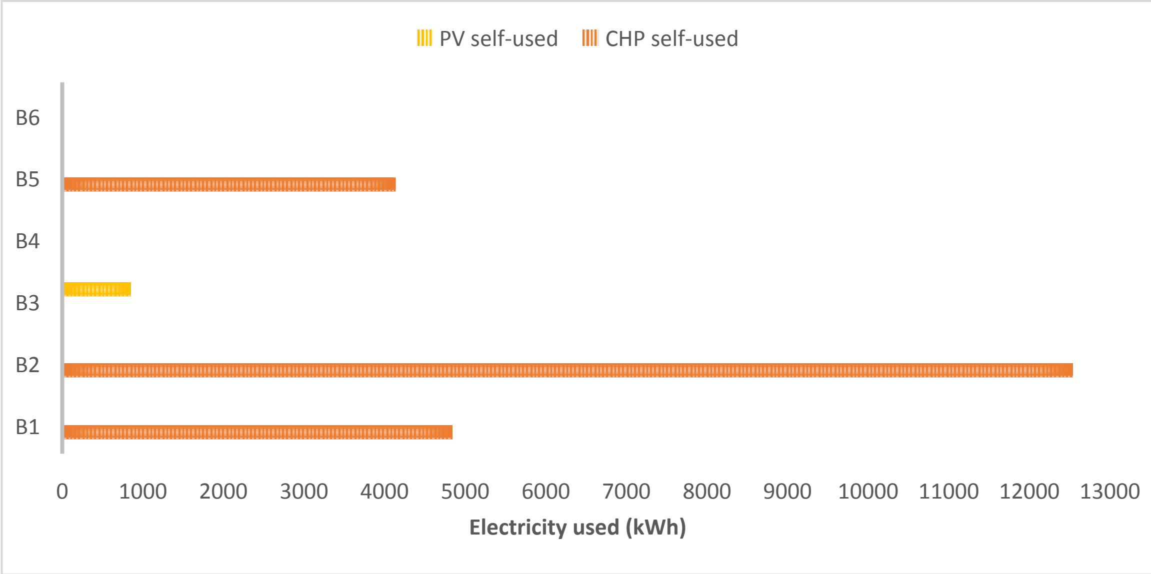


**(a)**

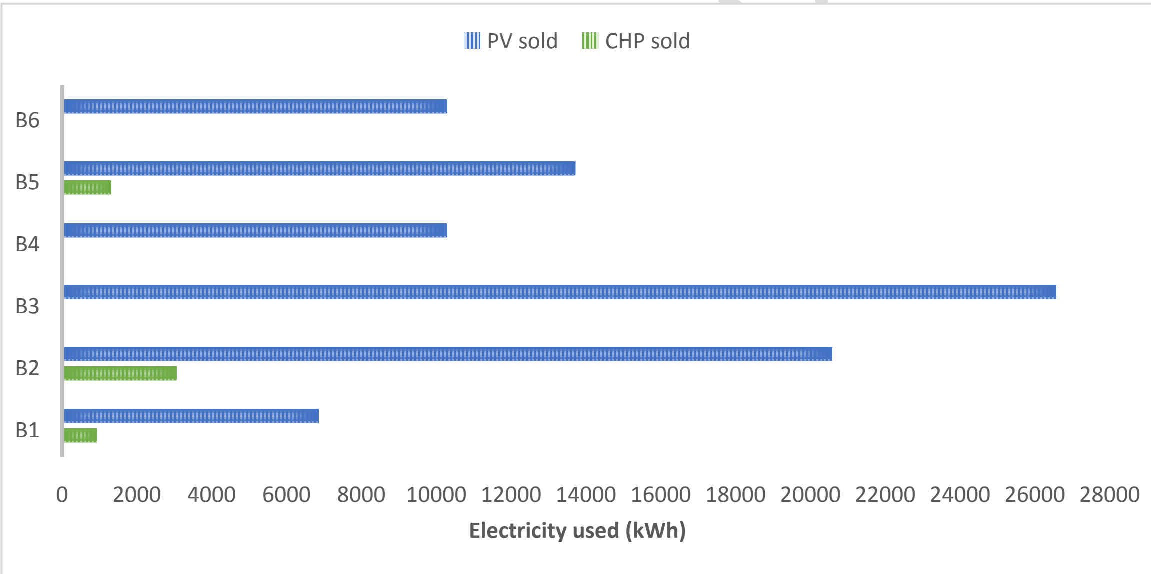


**(b)**

**Figure 14** Power energy balance throughout the year for net-zero energy district with storage based on (a) self-used and (b) sold energy

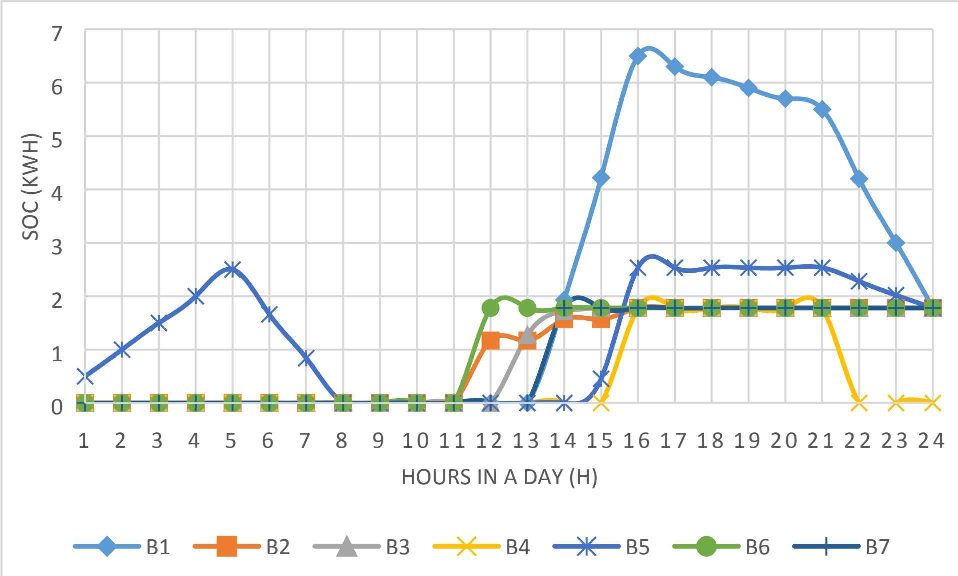


**Figure 15** Optimal state of charge for thermal storage inside all buildings in winter

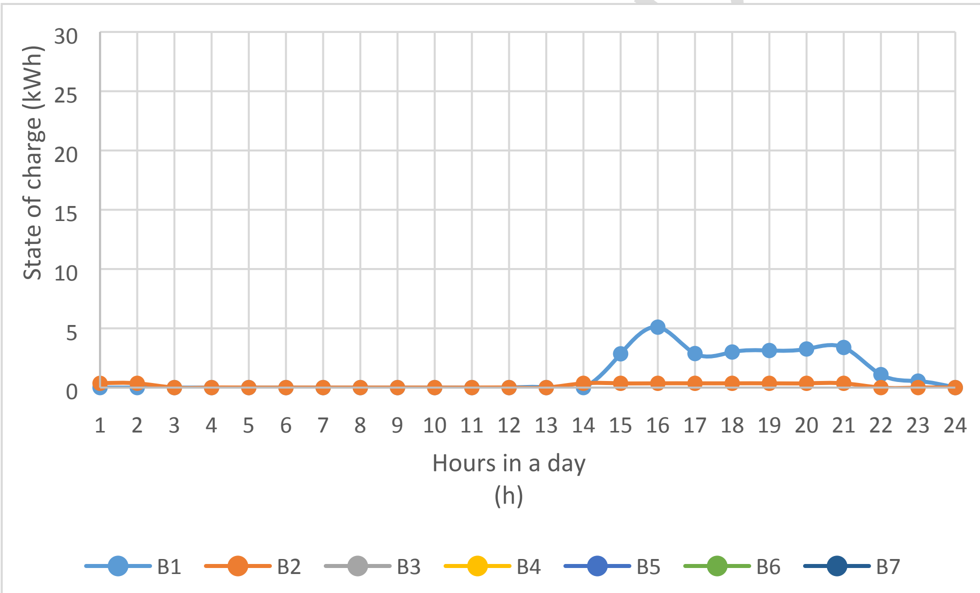


**Figure 16** Optimal state of charge for battery bank inside all buildings in mid-season

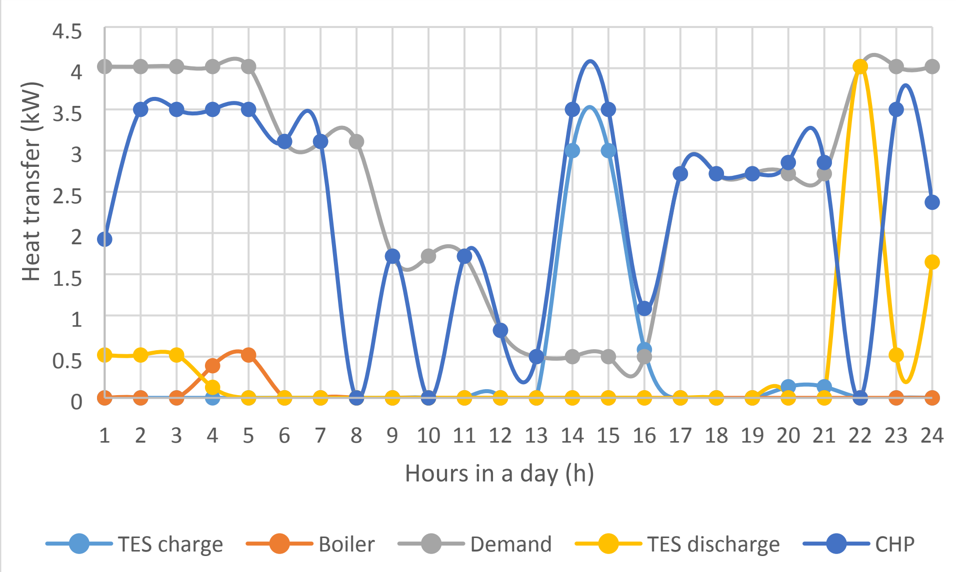


**Figure 17** Thermal energy balance of building B1 during a typical day in mid-season

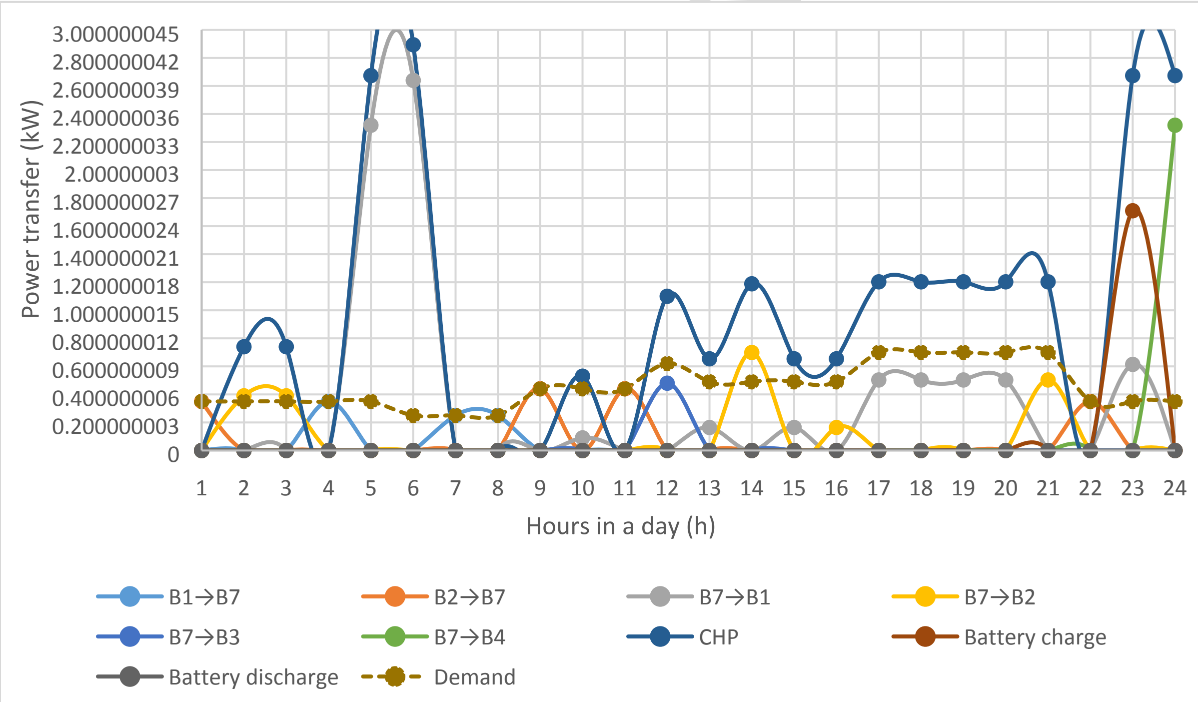


**Figure 18** Electricity balance of building B7 during a typical day in winter

## Tables

**Table 1** Definition of seasons and periods in the optimization model

<table>
<tr><td colspan="24">Seasons</td></tr>
<tr><td colspan="2">JAN</td><td colspan="2">FEB</td><td colspan="2">MAR</td><td colspan="2">APR</td><td colspan="2">MAY</td><td colspan="2">JUN</td><td colspan="2">JUL</td><td colspan="2">AUG</td><td colspan="2">SEP</td><td colspan="2">OCT</td><td colspan="2">NOV</td><td colspan="2">DEC</td></tr>
<tr><td colspan="4">Winter</td><td colspan="6">Mid-season</td><td colspan="8">Summer</td><td colspan="2"></td><td colspan="4">Winter</td></tr>
<tr><td colspan="24">Periods</td></tr>
<tr><td>1</td><td>2</td><td>3</td><td>4</td><td>5</td><td>6</td><td>7</td><td>8</td><td>9</td><td>10</td><td>11</td><td>12</td><td>13</td><td>14</td><td>15</td><td>16</td><td>17</td><td>18</td><td>19</td><td>20</td><td>21</td><td>22</td><td>23</td><td>24</td></tr>
<tr><td colspan="5">VI</td><td colspan="4">I</td><td colspan="3">II</td><td>III</td><td colspan="4">IV</td><td colspan="3">V</td><td colspan="4">VI</td></tr>
</table>

**Table 2** Component and network constraints imposed in the optimization model

| Remark | Formulation |
|---|---|
| Size of the auxiliary boilers is bounded according to market availability | $G_i^{B,lo} U_i \leq G_i^B \leq G_i^{B,up} U_i$ |
| Maximum number of CHP to be installed in each building | $\sum_k X_{i,k} \leq n^{CHP}$ |
| Maximum amount of heat production by CHP units in each building | $\sum_k G_k^{CHP} X_{i,k} \leq G_i^{CHP,max}$ |
| Available roof space for each building to install PV array | $A_i^{PV} \leq \frac{A_i^{PV,up}}{\cos\theta}$ |
| Heat can be exchanged between two buildings only in one direction | $Y_{i,j} + Y_{j,i} \leq 1$ |
| Selling and purchasing electricity for buildings is not permitted at the same time | $E_{i,s,t}^{grid} \leq E_{i,s,t}^{elec,tot}(1 - W_{i,s,t})$ |
| Selling electricity to the utility grid is bounded due to local/national regulations | $\sum_k E_{i,s,t,k}^{CHP,sel} + E_{i,s,t}^{PV,sel} \leq E_{i,s,t}^{sel,max} W_{i,s,t}$ |
| Generation of electricity by PV array is limited by incoming solar irradiation | $E_{i,s,t}^{PV,sel} + E_{i,s,t}^{PV,used} \leq A_i^{PV} \eta^{PV} S_{s,p}$ |
| Generation of electricity by PV array is limited by its capacity | $E_{i,s,t}^{PV,sel} + E_{i,s,t}^{PV,used} \leq A_i^{PV} G^{PV}$ |
| Optimal size of the CHP units should be selected according to the market availability | See figure 6. |
| Heat produced by the boiler should be less than its rated capacity at any time | $Q_{i,s,t}^{B} \leq G_i^B$ |
| Electricity produced by the CHP units should be less than its rated capacity at any time | $E_{i,s,t,k}^{CHP} \leq G_k^{CHP} X_{i,k}$ |
| Heat and electricity generated by CHP units are interconnected using heat to electricity ratio | $Q_{i,s,t,k}^{CHP} = E_{i,s,t,k}^{CHP} \zeta_k$ |
| Heat exchange among the buildings are restricted by the maximum capacity of pipeline | $Q_{i\to j,s,t} \leq Q_{i\to j,s,t}^{max} Y_{i,j}$ |
| Electricity exchange among the buildings is bounded | $E_{i\to j,s,t} \leq E_{i\to j,s,t}^{max} T_{i,j}$ |

| | |
|---|---|
| No heat circulation is allowed in the thermal distribution network | $V_j^O - V_i^O \leq 1 - (1 - Y_{i,j})\sum_i 1$ |
| Capacity of heat storage tank is bounded | $G_i^{HS,lo} B_i \leq G_i^{HS} \leq G_i^{HS,up} B_i$ |
| Heat delivered by the heat storage is lower than its capacity | $Q_{i,s,t}^{HS} \leq G_i^{HS}$ |
| Capacity of battery bank is bounded | $G_i^{BB,lo} R_i \leq G_i^{BB} \leq G_i^{BB,up} R_i$ |
| Power delivered by the battery bank is lower than its capacity | $E_{i,s,t}^{BB} \leq G_i^{BB}$ |

**Table 3** Heat load of each building in the district for each period and season (kW)

| | B7 | B6 | B5 | B4 | B3 | B2 | B1 | |
|---|---|---|---|---|---|---|---|---|
| Winter | 4.6 | 5.53 | 5.06 | 5.06 | 3.68 | 4.6 | 4.6 | **Period 1** |
| | 2.77 | 2.31 | 2.31 | 2.31 | 2.08 | 2.54 | 2.31 | **Period 2** |
| | 1.1 | 0.88 | 1.1 | 1.32 | 1.21 | 1.1 | 1.1 | **Period 3** |
| | 1.2 | 1.09 | 1.31 | 1.2 | 1.2 | 0.98 | 1.09 | **Period 4** |
| | 2.95 | 3.69 | 2.95 | 2.95 | 3.32 | 2.95 | 3.69 | **Period 5** |
| | 4.68 | 4.68 | 3.74 | 5.15 | 5.15 | 4.68 | 4.68 | **Period 6** |
| | | | | | | | | |
| Mid-season | 3.73 | 2.49 | 2.49 | 3.73 | 3.11 | 2.49 | 3.11 | **Period 1** |
| | 2.06 | 1.72 | 2.06 | 1.55 | 2.06 | 1.89 | 1.72 | **Period 2** |
| | 0.98 | 0.98 | 0.9 | 0.74 | 0.74 | 0.82 | 0.82 | **Period 3** |
| | 0.45 | 0.6 | 0.45 | 0.6 | 0.45 | 0.5 | 0.5 | **Period 4** |
| | 2.44 | 2.72 | 2.72 | 2.72 | 2.99 | 3.26 | 2.72 | **Period 5** |
| | 3.21 | 4.02 | 3.61 | 4.42 | 4.02 | 3.61 | 4.02 | **Period 6** |

**Table 4** Electricity load of each building in the district for each period and season (kW)

| | B7 | B6 | B5 | B4 | B3 | B2 | B1 | |
|---|---|---|---|---|---|---|---|---|
| Winter | 0.25 | 0.25 | 0.25 | 0.37 | 0.31 | 0.31 | 0.31 | **Period 1** |
| | 0.44 | 0.44 | 0.35 | 0.44 | 0.53 | 0.53 | 0.44 | **Period 2** |
| | 0.62 | 0.67 | 0.62 | 0.51 | 0.45 | 0.45 | 0.56 | **Period 3** |
| | 0.49 | 0.65 | 0.49 | 0.43 | 0.49 | 0.59 | 0.54 | **Period 4** |
| | 0.7 | 0.86 | 0.86 | 0.93 | 0.93 | 0.62 | 0.78 | **Period 5** |
| | 0.35 | 0.39 | 0.42 | 0.42 | 0.39 | 0.42 | 0.35 | **Period 6** |
| | | | | | | | | |
| Mid-season | 0.25 | 0.32 | 0.35 | 0.28 | 0.35 | 0.28 | 0.32 | **Period 1** |
| | 0.41 | 0.5 | 0.41 | 0.54 | 0.41 | 0.45 | 0.45 | **Period 2** |
| | 0.46 | 0.52 | 0.69 | 0.63 | 0.46 | 0.69 | 0.57 | **Period 3** |
| | 0.62 | 0.45 | 0.51 | 0.68 | 0.68 | 0.62 | 0.57 | **Period 4** |
| | 0.61 | 0.84 | 0.76 | 0.84 | 0.91 | 0.91 | 0.76 | **Period 5** |
| | 0.43 | 0.39 | 0.28 | 0.39 | 0.36 | 0.32 | 0.36 | **Period 6** |
| | | | | | | | | |
| Summer | 0.35 | 0.32 | 0.32 | 0.35 | 0.29 | 0.32 | 0.32 | **Period 1** |
| | 0.37 | 0.46 | 0.55 | 0.55 | 0.41 | 0.37 | 0.46 | **Period 2** |
| | 0.53 | 0.59 | 0.7 | 0.64 | 0.59 | 0.59 | 0.59 | **Period 3** |
| | 0.65 | 0.53 | 0.53 | 0.71 | 0.71 | 0.65 | 0.59 | **Period 4** |
| | 0.74 | 0.74 | 0.82 | 0.89 | 0.74 | 0.67 | 0.74 | **Period 5** |
| | 0.32 | 0.43 | 0.36 | 0.4 | 0.43 | 0.29 | 0.36 | **Period 6** |

**Table 5** Electricity selling and buying tariffs for each period and season (€/kWh) [30]

| Periods | Period 1 | Period 2 | Period 3 | Period 4 | Period 5 | Period 6 |
|---|---|---|---|---|---|---|
| **Purchase** | 0.1033 | 0.1230 | 0.1230 | 0.1230 | 0.1230 | 0.0659 |
| **Selling (PV)** | 0.55 | 0.55 | 0.55 | 0.55 | 0.55 | 0.55 |
| **Selling (CHP)** | 0.13 | 0.13 | 0.13 | 0.13 | 0.13 | 0.13 |

**Table 6.** Basic characteristics and capital costs of candidate equipment [32, 33, 34].

| Candidate technology | Capacity | Efficiency/Loss | Capital cost |
|---|---|---|---|
| **PV array** | 0.15 kW/m² | 12% | 4305 €/kW |
| **Heat storage** | 0 - 30 kWh | Charge: 95%<br>Discharge: 95% | 25 €/kWh |
| **Heating network** | 25 kW | Loss: 1% | 40 €/kW |
| **Battery bank** | 0 - 25 kWh | Charge: 95%<br>Discharge: 95% | 4000 €/kWh |

**Table 7** Available space in each building for PV installation

| Building | B1 | B2 | B3 | B4 | B5 | B6 | B7 |
|---|---|---|---|---|---|---|---|
| Roof area | 50 | 150 | 200 | 75 | 100 | 75 | 200 |

**Table 8** Technologies implemented and their sizes for the optimized net-zero energy district without storage

| | B1 | B2 | B3 | B4 | B5 | B6 | B7 |
|---|---|---|---|---|---|---|---|
| **CHP unit** | 10 kW | - | - | - | - | - | - |
| **Boiler** | - | - | - | - | - | - | - |
| **PV** | 50 $m^2$ | 150 $m^2$ | 200 $m^2$ | 75 $m^2$ | 100 $m^2$ | 75 $m^2$ | 200 $m^2$ |

**Table 9** Technologies implemented and their sizes for the optimized net-zero energy district with storage

| | B1 | B2 | B3 | B4 | B5 | B6 | B7 |
|---|---|---|---|---|---|---|---|
| **CHP unit** | 1 kW | 5 kW | - | - | 1 kW | - | 5 kW |
| **Boiler** | 1.18 kW | - | - | - | 0.77 kW | - | - |
| **TES** | 6.51 kW | 1.77 kW | 1.77 kW | 1.77 kW | 2.53 kW | 1.77 kW | 1.77 kW |
| **Battery** | 5.47 kW | 5.47 kW | 5.47 kW | 5.47 kW | 5.47 kW | 5.47 kW | 5.47 kW |
| **PV** | 50 $m^2$ | 150 $m^2$ | 200 $m^2$ | 75 $m^2$ | 100 $m^2$ | 75 $m^2$ | 200 $m^2$ |

**Table 10** Technologies implemented and their sizes for the optimized stand-alone district

| | B1 | B2 | B3 | B4 | B5 | B6 | B7 |
|---|---|---|---|---|---|---|---|
| **CHP unit** | 1 kW | 5 kW | - | - | 1 kW | - | 5 kW |
| **Boiler** | 1.18 kW | - | - | - | 0.77 kW | - | - |
| **TES** | 6.51 kW | 1.77 kW | 1.77 kW | 1.77 kW | 2.53 kW | 1.77 kW | 1.77 kW |
| **Battery** | 5.47 kW | 5.47 kW | 5.47 kW | 5.47 kW | 5.47 kW | 5.47 kW | 5.47 kW |
| **PV** | 50 $m^2$ | 150 $m^2$ | 200 $m^2$ | 75 $m^2$ | 100 $m^2$ | 75 $m^2$ | 200 $m^2$ |

with similar emission as net zero-energy district with storage

| | B1 | B2 | B3 | B4 | B5 | B6 | B7 |
|---|---|---|---|---|---|---|---|
| **CHP unit** | 1 kW | 1 kW | 1 kW | 1 kW | 1 kW | 1 kW | 1 kW |
| **Boiler** | 1.18 kW | 1.18 kW | 1.65 kW | 1.65 kW | 1.09 kW | 1.52 kW | 1.18 kW |
| **TES** | 5.46 kW | 4.45 kW | 5.94 kW | 5.94 kW | 1.48 kW | 5.45 kW | 4.45 kW |
| **Battery** | 5.05 kW | 5.05 kW | 5.05 kW | 5.05 kW | 5.05 kW | 5.05 kW | 5.05 kW |
| **PV** | - | - | - | - | - | - | - |

**Table 11** A cost and emission comparison among some important solutions for different scenarios

| **Scenario** | **Total annualized cost (€/year)** | **Total annual emission (kg/year)** |
|---|---|---|
| **Conventional district** | 12 000 | 24 300 |
| **Stand-alone (lowest cost)** | 8 600 | 24 500 |
| **Stand-alone (lowest emission)** | 10 500 | 19 500 |
| **Grid-connected without storage (net-zero energy)** | 0 | 22 500 |
| **Grid-connected without storage (lowest cost)** | -1 830 | 31 730 |
| **Grid-connected without storage (lowest emission)** | 1 325 | 20 700 |
| **Grid-connected with storage (net-zero energy)** | 0 | 20 800 |
| **Grid-connected with storage (lowest cost)** | -1 920 | 29 000 |
| **Grid-connected with storage (lowest emission)** | 1 418 | 18 500 |

***HIGHLIGHTS***

- A multi-level procedure is proposed for energy optimization of a new district;
- Type, size, and location of the equipment are all taken into account;
- An optimal design of a net-zero energy district is presented with and without storage;
- A case study with seven buildings is presented to show the applicability of methodology;
- The results are compared to the optimal design of a stand-alone district.